Comparison of time dependent fracture in viscoelastic and ductile solids

M.P. Wnuk*, M. Alavi[1], and A. Rouzbehani

College of Engineering and Applied Science, University of Wisconsin-Milwaukee, WI 53201, USA
[1] Finele Consulting Engineers, Inc., Hercules, CA 94547, USA

Effects of two parameters on enhancement of the time-dependent fracture manifested by a slow stable crack propagation that precedes catastrophic failure in ductile materials have been studied. One of these parameters is related to the material ductility (ρ) and the other describes the geometry (roughness) of crack surface and is measured by the degree of fractality represented by the fractal exponent α, or — equivalently — by the Hausdorff fractal dimension *D* for a self-similar crack. These studies of early stages of ductile fracture are preceded by a brief summary of modeling the phenomenon of delayed fracture in polymeric materials, sometimes referred to as "creep rupture". Despite different physical mechanisms involved in the preliminary stable crack extension and despite different mathematical representations, a remarkable similarity of the end results pertaining to the two phenomena of slow crack growth that occur either in viscoelastic or ductile media has been demonstrated.

Keywords: time-dependent fracture, crack propagation, stability of nonelastic fracture, viscoelastic solids, ductile solids, motion of cracks, process zone, unit step growth

DOI: 10.1134/S102995991201002X

1. Crack motion in a viscoelastic medium

In late sixties and early seventies of the past century a number of physical models and mathematical theories have been developed to provide a better insight and a quantitative description of the early stages of fracture in polymeric materials. In particular two phases of fracture initiation and subsequent growth have been considered: (i) the incubation phase during which the displacements of the crack surfaces are subject to creep process but the crack remains dormant; and (ii) slow propagation of a crack embedded in a viscoelastic medium. According to the linear theory of viscoelastic solids, the material response to the deformation process obeys the following constitutive relations

$$s_{ij}(t, \mathbf{x}) = \int_{0^-}^{t} G_1(t-\tau)\frac{\partial e_{ij}(\tau, \mathbf{x})}{\partial \tau}\,\mathrm{d}\tau,$$
$$s(t, \mathbf{x}) = \int_{0^-}^{t} G_2(t-\tau)\frac{\partial e(\tau, \mathbf{x})}{\partial \tau}\,\mathrm{d}\tau. \tag{1}$$

Here s_{ij} is the deviatoric part of the stress tensor, s denotes the spherical stress tensor, while $G_1(t)$ and $G_2(t)$ are time dependent relaxation moduli for shear and dilatation, respectively. The inverse relations read

$$e_{ij}(t, \mathbf{x}) = \int_{0^-}^{t} J_1(t-\tau)\frac{\partial s_{ij}(\tau, \mathbf{x})}{\partial \tau}\,\mathrm{d}\tau,$$
$$e(t, \mathbf{x}) = \int_{0^-}^{t} J_2(t-\tau)\frac{\partial s(\tau, \mathbf{x})}{\partial \tau}\,\mathrm{d}\tau. \tag{2}$$

Symbols e_{ij} and e are used to denote the deviatoric and spherical strain tensors and $J_1(t)$ and $J_2(t)$ are the two creep compliance functions. For a uniaxial state of stress these last two equations reduce to a simple form

$$\varepsilon(t) = \int_{0^-}^{t} J(t-\tau)\frac{\partial \sigma(\tau)}{\partial \tau}\,\mathrm{d}\tau. \tag{3}$$

The relaxation moduli $G_1(t)$, $G_2(t)$ and the creep compliance functions $J_1(t)$ and $J_2(t)$ satisfy the following integral equations

$$\int_{0^-}^{t} G_1(t-\tau)J_1(\tau)\,\mathrm{d}\tau = t,$$
$$\int_{0^-}^{t} G_2(t-\tau)J_2(\tau)\,\mathrm{d}\tau = t. \tag{4}$$

For a uniaxial state of stress these equations reduce to a single relation between the relaxation modulus $E_{\mathrm{rel}}(t)$ and the creep compliance function $J(t)$

* *Corresponding author*
Prof. Michael P. Wnuk, e-mail: mpw@uwm.edu

$$\int_{0^-}^{t} E_{\mathrm{rel}}(t-\tau)J(\tau)\,\mathrm{d}\tau = t. \tag{5}$$

Atomistic model of delayed fracture was considered by Zhurkov [1, 2], but this molecular theory had no great impact on the further development of the theories based in the continuum mechanics approaches. Inspired by Max Williams, W.G. Knauss in his doctoral thesis considered time dependent fracture of viscoelastic materials [3]. Similar research was done by [4] followed by simultaneous researches of Williams [5–7], Wnuk and Knauss [8], Field [9], Wnuk [10–17], and also by Knauss and Dietmann [18], Mueller and Knauss [19, 20], Graham [21, 22], Kostrov and Nikitin [23], Mueller [24], Knauss [25] and Schapery [26].

What follows in this section is an attempt to present a brief summary of the essential results, which have had a permanent impact on the development of the mechanics of time dependent fracture. After this review is completed we shall point out an interesting analogy of delayed fracture in polymers (intricately related to the ability to creep) with the "slow crack growth" (SCG) occurring in ductile solids due to the redistribution of strains within the yielded zone preceding the front of a propagating crack.

Two stages of delayed fracture in viscoelastic media, incubation and propagation, are described respectively by two governing equations: (1) Wnuk–Knauss equation and (2) Mueller–Knauss–Schapery equation. The duration of the incubation stage can be predicted from the Wnuk–Knauss equation

$$\Psi(t_1) = \frac{J(t_1)}{J(0)} = \left(\frac{K_{\mathrm{G}}}{K_0}\right)^2_{a=a_0=\mathrm{const}}. \tag{6}$$

Mueller–Knauss–Schapery equation relates the rate of crack growth $\overset{\circ}{a}$ to the applied constant load σ_0 and the material properties such as the unit step growth Δ, usually identified with the process zone size, and the Griffith stress $\sigma_{\mathrm{G}} = \sqrt{2E\gamma/(\pi a_0)}$, namely

$$\Psi\left(\frac{\Delta}{\dot{a}}\right) = \frac{J(\Delta/\dot{a})}{J(0)} = \left(\frac{K_{\mathrm{G}}}{K_0}\right)^2. \tag{7}$$

For a constant crack length equal the length of the initial crack a_0, the right hand side in (6) reduces to the square of the ratio of the Griffith stress to the applied stress

$$n = \left(\frac{\sigma_{\mathrm{G}}}{\sigma_0}\right)^2. \tag{8}$$

This quantity is sometimes referred to as "crack length quotient" — it determines how many times the actual crack is smaller than the critical Griffith crack. Therefore, the larger is the number *n*, the further away is the initial defect from the critical point of unstable propagation predicted for a Griffith crack embedded in a brittle solid. For large *n* the crack is too short to initiate the delayed fracture process, see expression (15) for the definition of the $n_{\max}$. Beyond $n_{\max}$ growth of the crack cannot take place. For $n > n_{\max}$ one can assume that these are stable cracks, which — according to the theory presented here — will never propagate. These are so-called "dormant cracks" that belong to a "no-growth" domain, see Appendix.

When crack length *a* is not constant, but it can vary with time $a = a(t)$, then the right side in (7) reads

$$\left(\frac{\sigma_{\mathrm{G}}}{\sigma_0}\right)^2 \frac{a_0}{a} = \frac{n}{x}. \tag{9}$$

Here *x* denotes the non-dimensional crack length, $x = a/a_0$. It is noteworthy that the physical meaning of the argument $\Delta/\dot{a}$ appearing in (7) is the time interval needed for the tip of a moving crack to traverse the process zone adjacent to the crack tip, say

$$\delta t = \Delta/\dot{a}. \tag{10}$$

The location of the process zone with respect to the cohesive zone which precedes a propagating crack is shown in Fig. 1.

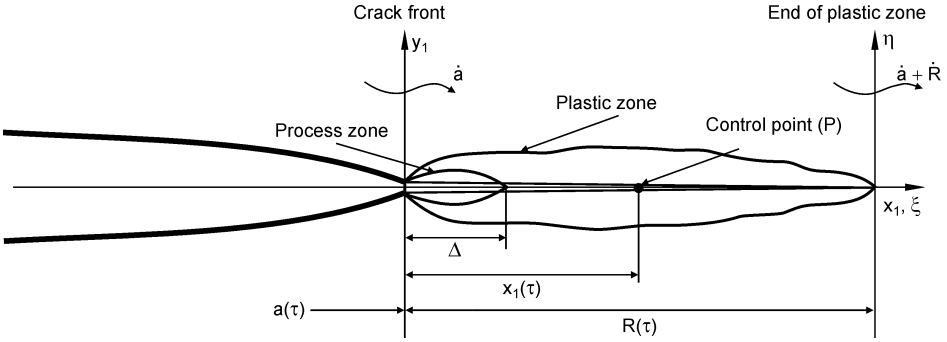

Fig. 1. Structured cohesive zone crack model of Wnuk [17, 27]. Note that of the two length parameters Δ and *R* the latter is time dependent analogous to length *a*, which denotes the length of the moving crack. Process zone size Δ is the material property and it remains constant during the crack growth process. Ratio R/Δ serves as a measure of material ductility; for $R/\Delta \gg 1$ material is ductile, while for $R/\Delta \geq 1$ material is brittle

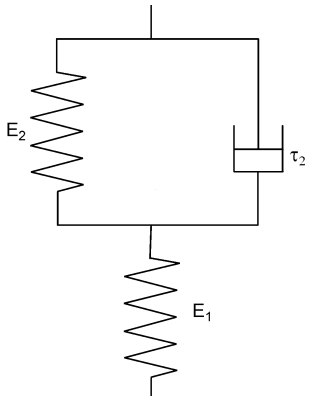

Fig. 2. Schematic diagram of the standard linear solid model

To illustrate applications of the equations (6) and (8) we shall use the constitutive equations valid for the standard linear solid, see Fig. 2. With β_1 denoting the ratio of the moduli E_1/E_2 the creep compliance function for this solid is given as

$$J(t)=\frac{1}{E_1}\left\{1+\beta_1\left[1-\exp(-t/\tau_2)\right]\right\}. \tag{11}$$

Therefore, the nondimensional creep compliance function $\Psi(t)=J(t)/J(0)$ reads

$$\Psi(t)=1+\beta_1\left[1-\exp(-t/\tau_2)\right]. \tag{12}$$

Substituting this expression into (6) one obtains

$$1+\beta_1\left[1-\exp(-t_1/\tau_2)\right]=n. \tag{13}$$

Solving for t_1 one obtains the following prediction for the incubation time valid for a material represented by standard linear solid

$$t_1=\tau_2\ln\left(\frac{\beta_1}{1+\beta_1-n}\right). \tag{14}$$

Inspection of (14) reveals that the quotient n should not exceed a certain limiting level

$$n_{\max}=1+\beta_1. \tag{15}$$

Physical interpretation of this relation can be stated as follows: for short cracks, when $n>n_{\max}$, there is no danger of initiating the delayed fracture process. These subcritical cracks are permanently dormant and they do not propagate.

Figure 3(*a*) illustrates the relationship between the incubation time and the loading parameter given either as n or $s\ (=1/\sqrt{n}=\sigma_0/\sigma_G)$. Figure 3(*b*) shows an analogous relation between the time used in the process of crack propagation and the loading parameter s. Note that the incubation time is expressed in units of the relaxation time τ_2, while the time measured during the crack propagation phase of the delayed fracture is expressed in units of τ_2/δ, in where the constant δ contains the initial crack length a_0 and the characteristic material length Δ, cf. (18). When the variable s is used on the vertical axis and the pertinent function is plotted against the logarithm of time, then it is seen that a substantial portion of the curve appears as a straight line. This confirms the experimental results of Knauss and Dietmann [18] used also by Schapery [26] and Mohanty [28].

To describe motion of a crack embedded in viscoelastic solid represented by the standard linear model one needs to insert (11) into the governing equation (7). The equation of motion reads then

$$1+\beta_1\left[1-\exp(-\delta t/\tau_2)\right]=\frac{n}{x}. \tag{16}$$

Solving it for the time interval $\delta t/\tau_2=\Delta/(\dot{a}\tau_2)$ yields

$$\frac{\Delta}{\tau_2\dot{a}}=\ln\left(\frac{\beta_1}{1+\beta_1-n/x}\right). \tag{17}$$

It is seen from (17) that for the motion to exist, the quotient n should not exceed the maximum value defined by Eq. (15). For $n>n_{\max}$ the cracks are too small to propagate.

If nondimensional notation for the length and time variables is introduced

$$\delta=\Delta/a_0,\quad \theta=t/\tau_2, \tag{18}$$

the left hand side of (17) can be reduced as follows

$$\frac{\delta t}{\tau_2}=\frac{\Delta}{\tau_2\dot{a}}=\frac{\Delta}{\dfrac{\mathrm{d}(xa_0)}{\mathrm{d}(\theta\tau_2)}\tau_2}=\frac{\Delta/a_0}{\mathrm{d}x/\mathrm{d}\theta}. \tag{19}$$

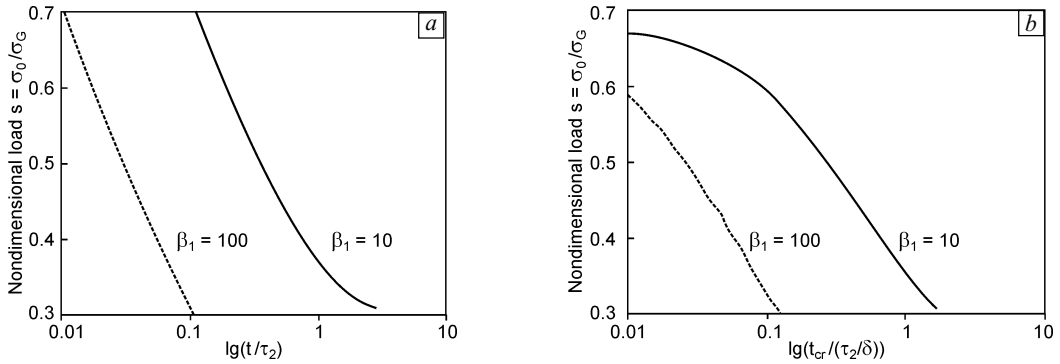

Fig. 3. Logarithm of the incubation time in units of τ_2 shown as a function of the loading parameter s for two different values of the material constant $\beta_1=E_1/E_2$ (*a*). Logarithm of the time-to-failure used during the crack propagation phase, in units of τ_2, shown as a function of the loading parameter s for two different values of the material constant $\beta_1=E_1/E_2$ (*b*)

When this is inserted into (17) and with $\delta = \Delta/a_0$, the following differential equation results

$$\frac{dx}{d\theta} = \delta\left[\ln(\beta_1/(1+\beta_1 - n/x))\right]^{-1} \tag{20}$$

or, after separation of variables

$$(\delta)d\theta = \ln(\beta_1/(1+\beta_1 - n/x))\,dx. \tag{21}$$

Motion begins at the first critical time t_1, which designates the end of the incubation period. Therefore, the lower limit for the integral applied to the left hand side of (21) should be $\theta_1 = t_1/\tau_2$, while the upper limit is the current nondimensional time $\theta = t/\tau_2$. The corresponding upper limit to the integral on the right hand side of (21) is the current crack length $x = a/a_0$, while the lower limit is one. Upon integration one obtains

$$\int_{t_1/\tau_2}^{t/\tau_2} d\theta = \left(\frac{1}{\delta}\right)\int_1^x \ln(\beta_1/(1+\beta_1 - n/z))\,dz. \tag{22}$$

The resulting expression relates the crack length x to time t, namely

$$t - t_1 = = \left(\frac{\tau_2}{\delta}\right)\int_1^x \ln(\beta_1/(1+\beta_1 - n/z))\,dz. \tag{23}$$

If the closed form solution for the integral in (23) is used, then this formula can be cast in the following final form

$$t = t_1 + \left(\frac{\tau_2}{\delta}\right)\left\{x\ln\left[\frac{x\beta_1}{(1+\beta_1)x - n}\right] + \right.$$
$$\left. + \frac{n}{1+\beta_1}\ln\left[\frac{(1+\beta_1)x - n}{1+\beta_1 - n}\right] + \ln\left(\frac{1+\beta_1 - n}{\beta_1}\right)\right\}. \tag{24}$$

This equation has been used in constructing the graphs shown in Fig. 4. At $\beta_1 = 10$ three values of n have been used (4.00, 6.25 and 8.16, which corresponds to the following values of s: 0.5, 0.4 and 0.35). It can be observed that at x approaching n the phase of the slow crack propagation is transformed into unrestrained crack extension tantamount to the catastrophic fracture. The point in time, at which this transition occurs, can be easily seen on the horizontal axis of Fig. 4. This point of transition into unstable propagation can also be predicted from (24); substituting n for x we obtain the time to fracture

$$t_2 = \left(\frac{\tau_2}{\delta}\right)\left\{\frac{n}{1+\beta_1}\ln\left[\frac{\beta_1 n}{1+\beta_1 - n}\right] + \right.$$
$$\left. + \ln\left[\frac{1+\beta_1 - n}{\beta_1}\right]\right\}. \tag{25}$$

If the incubation time t_1 given by (14) is now added to (25), one obtains the total life time of the component, namely

$$T_{cr} = t_1 + t_2 = \tau_2\ln\left(\frac{\beta_1}{1+\beta_1 - n}\right) +$$
$$+\left(\frac{\tau_2}{\delta}\right)\left\{\frac{n}{1+\beta_1}\ln\left[\frac{\beta_1 n}{1+\beta_1 - n}\right] + \ln\left[\frac{1+\beta_1 - n}{\beta_1}\right]\right\}. \tag{26}$$

Summarizing the results of this section we can state that the delayed fracture in a viscoelastic solid can be mathematically represented by four expressions:

– time of incubation t_1 given by (14) for standard linear model,

– equation of motion given by (24) for the same material model and defining x as a function of time, $x = x(t)$,

– time to fracture t_2 due to crack propagation given by (25),

– lifetime T_{cr} equal to the sum $t_1 + t_2$, as given by Eq. (26). It is noted that while the first term in the expression (26) involves the relaxation time, material constant β_1 and the quotient n, the second term in (26) contains also the internal structural constant δ. It is also noted that for the quotient n approaching one, both terms in (26) are zero, while for n exceeding n_{max}, the expression looses the physical sense (since in that case there is no propagation). With the constant δ being on the order of magnitude varying within the range 10^{-3} to 10^{-6} the second term in (26) is substantially greater than the first term which represents the incubation time, see also Appendix.

For $\beta_1 = 10$ and three different levels of n, the resulting functional relationships between the crack length x and time t are shown in Fig. 4 along with the values of the incubation times, expressed in units of τ_2, and the times-to-failure expressed in units of τ_2/δ. A numerical example is given in the Appendix.

Example described here, involving the standard linear solid, serves as an illustration of the mathematical procedures necessary in predicting the delayed fracture in polymeric materials. Knauss and Dietmann [18] and Schapery [26] have shown how the real viscoelastic materials, for

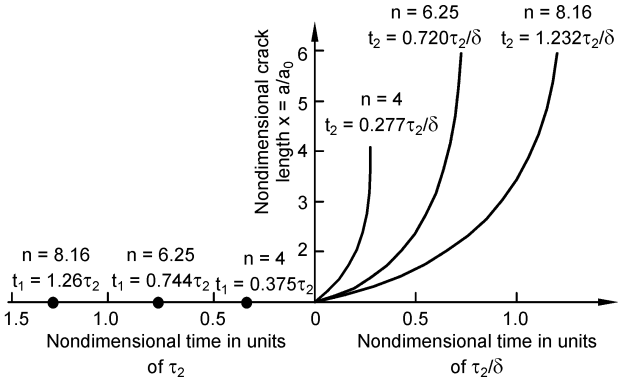

Fig. 4. Slow crack propagation occurring in a linear viscoelastic solid represented by the standard linear model depicted in Fig. 2 at $\beta_1 = 10$. Crack length is shown as a function of time; points marked on the negative time axis designate the incubation times corresponding to the given level of the applied constant load n and expressed in units of τ_2. The time interval between the specific point t_1 and the origin of the coordinates provides the duration of the incubation period. Crack propagation begins at $t = 0$. Symbol t_2 denotes time-to-failure, which is the time used during the quasi-static phase of crack extension and it is expressed in units of τ_2/δ. Constant δ is related to the characteristic material length, the so-called "unit growth step" Δ

which the relaxation modulus $G(t)$ and the creep compliance function $J(t)$ are measured (or calculated from equation (4)) and then used in the governing equations of motion discussed above can provide a good approximation of the experimental data.

2. Quasi-static stable crack propagation in ductile solids

Crack embedded in a ductile material will tend to propagate well below the threshold level indicated by the ASTM standards. This phenomenon of slow crack growth (SCG) is sometimes referred to as "subcritical" or "quasi-static" crack propagation and it is caused by the redistribution of elasto-plastic strains induced at the front of the propagating crack. The higher is the ductility of the material, the more pronounced is the preliminary crack extension associated with the early stages of fracture. For brittle solids this effect vanishes.

Ductility of the material is defined as the ratio of two characteristic strains, namely

$$\rho = \frac{\varepsilon^{\mathrm{f}}}{\varepsilon_{\mathrm{Y}}} = 1 + \frac{\varepsilon^{\mathrm{f}}_{\mathrm{pl}}}{\varepsilon_{\mathrm{Y}}}. \tag{27}$$

Here ε^{f} denotes strain at fracture, and it can be expressed as the sum of the yield strain ε_{Y} and the plastic component of the strain at fracture $\varepsilon^{\mathrm{f}}_{\mathrm{pl}}$. We will refer to the material property defined by (27) as ductility index and we shall relate it to the parameters inherent in the structured cohesive zone crack model, cf. Wnuk [17, 26] — see also Fig. 1. According to Wnuk and Mura [29, 30] the relation is as follows

$$\rho = \frac{R_{\mathrm{ini}}}{\Delta}. \tag{28}$$

Here the symbol R_{ini} denotes the length of the cohesive zone at the onset of crack growth, while Δ is the process zone size or the so-called "unit growth step" for a propagating crack. In order to mathematically describe motion of a quasi-static crack one needs to know the distribution of the opening displacement within the cohesive zone of the crack shown in Fig. 1. When the cohesive zone is much smaller than the crack length (this is the so-called Barenblatt's condition) according to Rice [31] and Wnuk [27] this distribution is established as follows

$$u_y(x_1, R) = \frac{4\sigma_{\mathrm{Y}}}{\pi E_1}\left\{\sqrt{R(R-x_1)} - \right.$$

$$\left. - \frac{x_1}{2}\ln\left[\frac{\sqrt{R}+\sqrt{R-x_1}}{\sqrt{R}-\sqrt{R-x_1}}\right]\right\}. \tag{29}$$

Here x_1 denotes the distance measured from the physical crack tip, E_1 is the Young modulus E for the case of plane stress, while for the plane strain it is $E(1-\nu^2)^{-1}$ where ν is the Poisson ratio. Symbol σ_{Y} denotes the yield stress present within the end zone. For a moving crack both x_1 and R are certain functions of time — or, equivalently — of the crack length a, which can be used here as a time-like variable. In agreement with Wnuk's "final stretch criterion", cf. Wnuk [17, 27], two adjacent states of the time-dependent structured cohesive zone should be examined simultaneously, as shown in Fig. 5. At the instant t (state 2 in Fig. 5) the opening displacement $u_y(x_1(t), R(t))$ measured at the control point P, say $u_2(P)$, equals

$$u_2(P) = \frac{4\sigma_0}{\pi E_1}[R]_{x_1=0} = \frac{4\sigma_0}{\pi E_1}\left\{[R]_{x_1=\Delta} + \frac{\mathrm{d}R}{\mathrm{d}a}\Delta\right\}. \tag{30}$$

Expansion of the variable $R(x_1)$ into a Taylor series is justified, since both states considered are in close proximity. For simplicity the entity $[R]_{x_1=\Delta}$ shall be referred to as $R(\Delta)$. Note that at the preceding instant "t–δt" then (state 1 in Fig. 5) the vertical displacement u_y within the cohesive zone, measured at the control point P, located at $x_1 = \Delta$ for state 1, equals

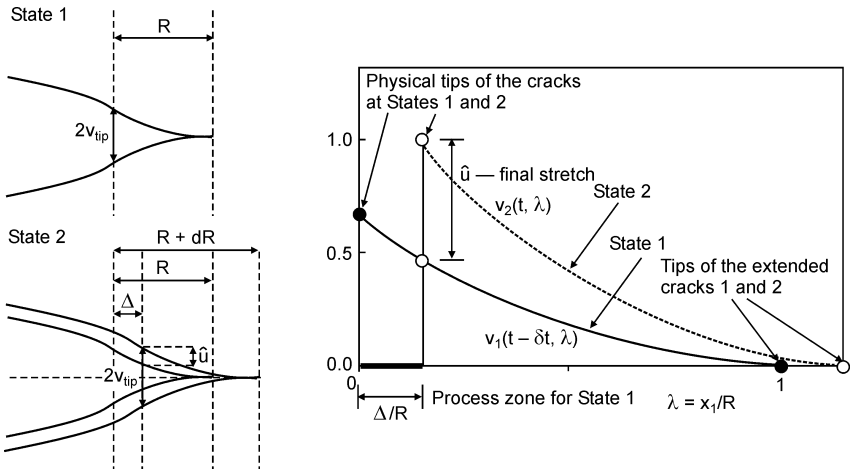

Fig. 5. Distribution of the COD within the cohesive zone corresponding to two subsequent states represented by instants t and t–δt in the course of quasi-static crack extension as required in Wnuk's criterion of delta COD; $[v_2(t) - v_1(t-\delta t)]_p$ = final stretch

$$u_1(P)=\frac{4\sigma_0}{\pi E_1}\left\{\sqrt{R(\Delta)(R(\Delta)-\Delta)}-\right.$$
$$\left.-\frac{\Delta}{2}\ln\left[\frac{\sqrt{R(\Delta)}+\sqrt{R(\Delta)-\Delta}}{\sqrt{R(\Delta)}-\sqrt{R(\Delta)-\Delta}}\right]\right\}. \quad (31)$$

According to Wnuk's "delta COD" or "final stretch" criterion for crack motion to occur it is necessary that the difference between (30) and (31) is maintained constant and equal to the material parameter $\bar{\delta}/2$, where $\bar{\delta}$ is the final stretch regarded invariant during the crack growth process. Note that a similar requirement is postulated for the size of the process zone or unit growth step, $\Delta = \text{const}$. Therefore, the final stretch criterion reads

$$u_2(P)-u_1(P)=\bar{\delta}/2. \quad (32)$$

Substituting (30) and (31) into the criterion of subcritical motion (32) and naming $R(\Delta)$ by R, one obtains the following differential equation

$$R+\Delta\frac{\mathrm{d}R}{\mathrm{d}a}-\sqrt{R(R-\Delta)}+$$
$$+\frac{\Delta}{2}\ln\left[\frac{\sqrt{R}+\sqrt{R-\Delta}}{\sqrt{R}-\sqrt{R-\Delta}}\right]=\frac{\bar{\delta}}{2}\left(\frac{\pi E_1}{4\sigma_Y}\right). \quad (33)$$

We note that while both $\bar{\delta}$ and Δ are constant, the entity R is a certain unknown function of the crack length a. Using the nondimensional length of the cohesive zone, Y and the nondimensional crack length X

$$Y=\frac{R}{R_{\text{ini}}},\quad X=\frac{a}{R_{\text{ini}}} \quad (34)$$

and denoting the group of material constants on the right hand side of (33) by M and referring to it in the sequel as "tearing modulus"

$$M=\frac{\bar{\delta}}{2}\left(\frac{\pi E_1}{4\sigma_Y}\right), \quad (35)$$

we rewrite the governing differential equation (33) in this form

$$\frac{\mathrm{d}Y}{\mathrm{d}X}=M-\rho Y+\sqrt{\rho Y(\rho Y-1)}-$$
$$-\frac{1}{2}\ln\left[\frac{\sqrt{\rho Y}+\sqrt{\rho Y-1}}{\sqrt{\rho Y}-\sqrt{\rho Y-1}}\right]. \quad (36)$$

This equation can be further reduced if it is assumed that we focus the attention on the ductile material behavior, when $R \gg \Delta$, and therefore consider the case when the ductility index ρ substantially exceeds one. Physically it means that the process zone Δ is much smaller than the length of the cohesive zone. With such an assumption and some algebraic manipulations involving expansion of the pertinent functions into power series one may reduce the right hand side of (36) to the following simple form, cf. Wnuk [17, 27] and Rice et al. [32–34]

$$\frac{\mathrm{d}Y}{\mathrm{d}X}=M-\frac{1}{2}-\frac{1}{2}\ln(4\rho Y). \quad (37)$$

Slow crack growth is possible only if the initial slope of (37) is positive, i.e.,

$$\left[\frac{\mathrm{d}Y}{\mathrm{d}X}\right]_{Y=1}\geq 0. \quad (38)$$

This condition imposes a certain restriction on the tearing modulus M. For motion to take place M must be greater than a certain minimum tearing modulus, i.e.,

$$M_{\min}=\frac{1}{2}+\frac{1}{2}\ln(4\rho). \quad (39)$$

To illustrate applications of the governing equation (37) we shall assume in what follows that the tearing modulus $M(\rho)$ is 10 % higher than the minimum modulus defined by (39)

$$M(\rho)=1.1\left[\frac{1}{2}+\frac{1}{2}\ln(4\rho)\right]. \quad (40)$$

Now we focus attention on the differential equation (37) amended by the condition (40), namely

$$\frac{\mathrm{d}Y}{\mathrm{d}X}=M(\rho)-\frac{1}{2}-\frac{1}{2}\ln(4\rho Y). \quad (41)$$

It is noteworthy that according to the cohesive crack model the length R differs only by a multiplicative constant from Rice's J-integral and from the Wells [35] opening displacement", COD. Denoting the COD by δ_{tip}, we recall the following well-known relations valid for a cohesive crack model under the restriction of small scale yielding when the Barenblatt condition applies

$$J=\sigma_Y\delta_{\text{tip}},\quad \delta_{\text{tip}}=\left(\frac{8\sigma_Y}{\pi E_1}\right)R,\quad J=\left(\frac{8\sigma_Y^2}{\pi E_1}\right)R, \quad (42)$$
$$\beta(a)=\frac{\sigma(a)}{\sigma_Y}=\frac{2}{\pi}\sqrt{\frac{2R(a)}{a}}=\frac{2}{\pi}\sqrt{\frac{2Y(X)}{X}}.$$

The last equation in (42) represents the Dugdale relation between the length of the cohesive zone R and the applied load σ valid for a propagating crack for which both σ and R are certain functions of the crack length, while R is subjected to the Barenblatt condition $R \ll a$. When physical interpretation is applied to the equations listed in (42), one comes to a conclusion that the material resistance $J_R(a)$ due to continuing crack growth can be readily represented by the resistance curve $R = R(a)$, or $Y = Y(X)$. Denoting the ratio σ/σ_Y by β, we rewrite the last of the equations (42) as follows

$$\beta(X)=\frac{2}{\pi}\sqrt{\frac{2Y(X)}{X}}. \quad (43)$$

Of course, β defined by (43) is a function of X. Let us now denote the right hand side of the governing differential equation of a moving crack by $F(Y, \rho)$. Equation (41) thus reads

$$\frac{\mathrm{d}Y}{\mathrm{d}X}=F(Y,\rho). \quad (44)$$

Solution of (44) is readily obtained by the separation of variables followed by the integration, namely

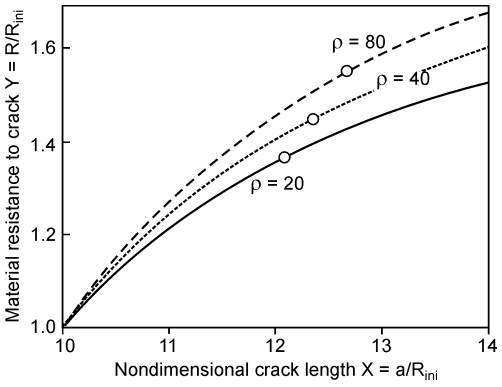

Fig. 6. Material resistance curves obtained for three different levels of material ductility ρ = 20, 40 and 80 and for the initial crack length $a_0 = 10R_{\text{ini}}$. Points of terminal instability for each case are marked with little circles. Compared to a brittle solid, for which ductility index approaches one, the following increases in the effective material toughness at the transition to catastrophic fracture are observed: 36.6 % at ρ = 20, 45.2 % at ρ = 40 and 54.2 % at ρ = 80

$$X(Y) = X_0 + \int_1^Y \frac{1}{F(z,\rho)}\,\mathrm{d}z. \tag{45}$$

Examples of the material resistance curves $Y = Y(X)$, or $J_R = J_R(a)$, that result from (45) are shown in Fig. 6. It is seen that the level of material ductility ρ has a substantial influence on the slope and shape of such material resistance curves. Figure 7 shows the graphs illustrating dependence of the loading parameter β on the current crack length at various values of the ductility index ρ. Equation (43) has been used to construct these curves. At a certain value of X each such "beta-curve" attains a maximum. When the slope $\mathrm{d}\beta/\mathrm{d}X$ approaches zero, the stable crack growth can no longer be sustained. Effects of the specimen geometry and

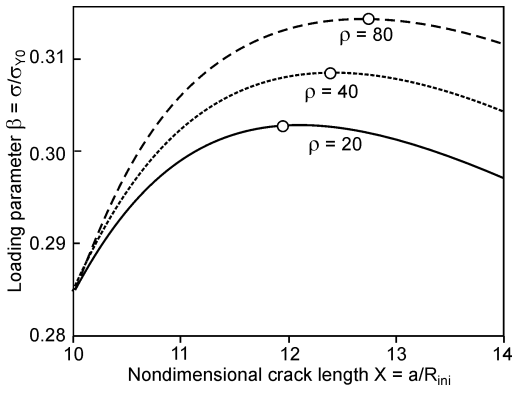

Fig. 7. Nondimensional loading parameter $\beta\ (=\sigma/\sigma_{\text{Y}})$ shown as a function of the current crack length $X = a/R_{\text{ini}}$. During the quasi-static crack extension the applied load increases with an increasing crack length up to the point of maximum on the beta-curve. At this point the slow crack growth process ends and the transition to unstable (catastrophic) crack propagation takes place. Thus, the curves shown in the figure loose their physical meaning beyond the points of maxima. Observed increases in the loading parameter β, compared to the case of ideally brittle solid, are as follows: 4.4 % for ρ = 20, 8.3 % for ρ = 40 and 10.4 % for ρ = 80

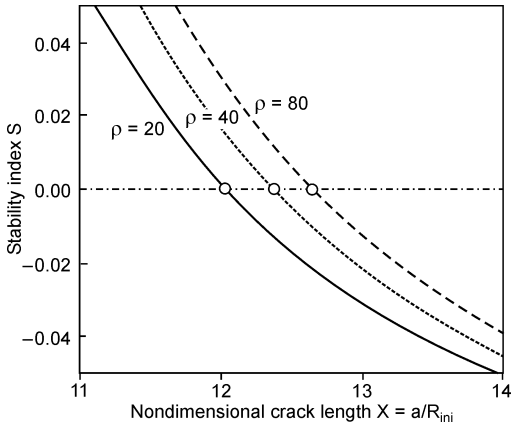

Fig. 8. Stability index S shown as a function of the current length X of the propagating crack. It is noted that the function S passes through zero at the values of length X exactly coinciding with the location of the maxima observed on the beta-curves. The predicted increases in the crack length occurring due to the preliminary slow crack growth are as follows: 20.8 % for ρ = 20, 23.7 % for ρ = 40, and 26.5 % for ρ = 80

loading configuration on the instabilities in fracture governed by equations (44) and (45) were studied by Rouzbehani and Wnuk [36]. Some other aspects of the structured cohesive crack model and Wnuk's criterion for subcritical crack growth were described in Wnuk [37–39].

Quasi-static crack extension is viewed as a sequence of the local instability states. Attainment of the terminal instability state, which is tantamount to the catastrophic fracture, is seen as the termination of the slow crack growth process. There are several techniques to establish the exact location (load and crack length) of the terminal instability state. Perhaps the simplest approach is to seek the maximum on the beta-curve. To do just that let us rewrite (43) as follows

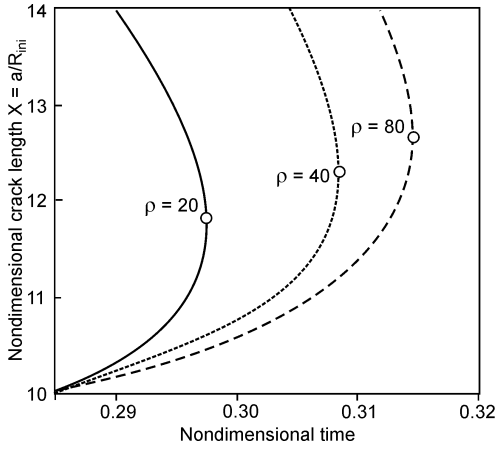

Fig. 9. Crack length X during the quasi-static crack growth process shown as a function of the nondimensional time. In order to construct these graphs a constant rate of load increase was assumed. At the points where the slopes of these curves approach infinity the slow crack extension undergoes a transition into unstable (catastrophic) crack propagation. Note that this transition occurs at the values of X corresponding to the maxima on the beta-curves shown in Fig. 7, or — equivalently — the zeros of the S-functions shown in Fig. 8

$$\beta^2 = \left(\frac{4}{\pi^2}\right)\frac{2Y}{X}. \tag{46}$$

Differentiating both sides with respect to Y one gets

$$2\beta\,\mathrm{d}\beta = \frac{8}{\pi^2}\frac{X-(\mathrm{d}X/\mathrm{d}Y)Y}{X^2}\,\mathrm{d}Y. \tag{47}$$

Hence

$$\beta\frac{\mathrm{d}\beta}{\mathrm{d}Y} = \frac{4}{\pi^2}\left(\frac{1}{X}\right)\left[1-\frac{(\mathrm{d}X/\mathrm{d}Y)Y}{X}\right]. \tag{48}$$

In order to convert this expression to $\mathrm{d}\beta/\mathrm{d}X$ one needs to multiply it by $\mathrm{d}Y/\mathrm{d}X$ defined by (44), which yields

$$\frac{\mathrm{d}\beta}{\mathrm{d}X} = \frac{4}{\pi^2}\frac{1}{\beta X}\left[F(Y,\rho)-\frac{Y}{X}\right]. \tag{49}$$

For convenience we shall refer to the quantity proportional to the derivative $\mathrm{d}\beta/\mathrm{d}X$ as the "stability index" $S = S(X)$, namely

$$S(X) = \frac{\pi^2}{4}X\beta\frac{\mathrm{d}\beta}{\mathrm{d}X},\quad S(X) = F(Y,\rho)-\frac{Y}{X}. \tag{50}$$

Examples of the plots S vs. X are given in Figure 8. As can be readily seen all curves intersect the axis $S = 0$, and it is easy to read (or evaluate numerically) those zero points present in the stability indices diagrams. The results $X_{\max}$, $Y_{\max}$ and $\beta_{\max}$ provide the coordinates characterizing the terminal instability states. It should be noted that the first term in the expression for the stability index S in (50) is proportional to the rate at which energy is absorbed by the ductile material, while the second term is proportional to the rate at which energy is supplied by the external force. Both terms can be shown to be related to the second derivatives of the potential energy of a solid weakened by a crack and subjected to certain kind of external loading configuration corresponding to either "fixed grips" or "constant load" boundary condition, cf. the Appendix.

In order to demonstrate the crack propagation process the diagrams shown in Fig. 7 have been re-plotted in the way shown in Fig. 9. Here the vertical axis represents the current crack length, while the horizontal axis shows a nondimensional variable proportional to time. To make these graphs as simple as possible a constant rate of load increase has been assumed. The graphs shown in this figure are remarkably similar to the graphs shown in Fig. 4 obtained for a crack propagating through a viscoelastic medium.

Despite very different physical interpretation of the mechanisms that make slow crack growth possible in the two considered cases, viscoelastic and ductile media, the end results are strikingly similar.

3. Effect of crack surface roughness on the extent of the quasi-static crack growth. Fractal fracture mechanics

For almost all materials it is necessary to account for the roughness of the crack surfaces. Mathematically this can be achieved by application of the fractal model of a crack, cf. Wnuk and Yavari [40–43] and Khezrzadeh et al. [44]. The degree of fractality — proportional to the degree of roughness of the crack surfaces — is suitably measured by the fractal exponent α, which appears in the expression for the near-tip stress field associated with a fractal crack, namely

$$\sigma_{ij} \sim r^{-\alpha}. \tag{51}$$

The exponent α is related to the Hausdorff measure D of the fractal used to represent a self-similar crack

$$D = 2(1-\alpha). \tag{52}$$

Variation of the fractal dimension D from 1 (smooth crack) to 2 (two-dimensional void) corresponds to the variation of the exponent α from $1/2$ to 0. Therefore, for $\alpha = 1/2$ expression (51) yields the relation well-known in the linear elastic fracture mechanics (LEFM), while for the other extreme of α approaching zero, the singularity in (51) disappears. Wnuk and Yavari model [40] of an a crack embedded in the stress field due to a fractal geometry of the crack applies to the range of α close to 0.5 — corresponding to the range of the fractal dimension D close to 1.

In what follows we shall study the effect of the degree of fractality (measured either by α or by D) on the quasi-static crack extension, which precedes catastrophic fracture. We shall apply the formula for the opening displacement within the cohesive zone associated with a structured cohesive crack model of Wnuk and extended to the fractal geometry, namely

$$u_y(x_1,R) = \frac{4\sigma_Y}{\pi E_1}\kappa(\alpha)\left\{\sqrt{R^{\mathrm{f}}(R^{\mathrm{f}}-x_1)} - \frac{x_1}{2}\ln\left[\frac{\sqrt{R^{\mathrm{f}}}+\sqrt{R^{\mathrm{f}}-x_1}}{\sqrt{R^{\mathrm{f}}}-\sqrt{R^{\mathrm{f}}-x_1}}\right]\right\}, \tag{53}$$

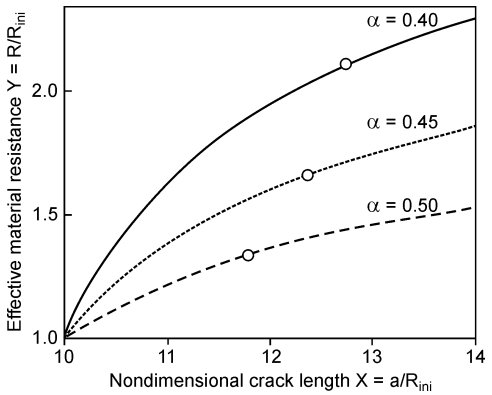

Fig. 10. Material resistance curves $R(a)/R_{\mathrm{ini}}$ obtained for a smooth crack (the lowest curve, $\alpha = 0.5$) and two fractal cracks defined by the fractal exponent α equal 0.45 (or $D = 1.1$) and $\alpha = 0.40$ (or $D = 1.2$). It is noted that increasing roughness of the crack surfaces, measured either by α, or the dimension D, enhances the effects of the slow crack growth on the effective material resistance. When the effective material resistance is compared with the one obtained for a smooth crack, one observes 57.4 % increase for the fractal crack described by $\alpha = 0.40$ and 26.6 % for the fractal crack with $\alpha = 0.45$

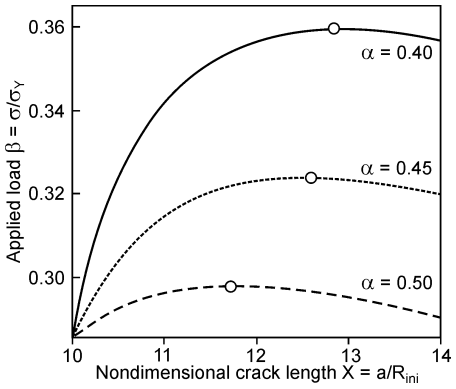

Fig. 11. Applied load shown as function of the current crack length. The lowest curve corresponds to a smooth crack, while the other two describe fractal cracks with rough surfaces. Degree of fractality is determined by the exponent α or the dimension D; for the intermediate curve $\alpha = 0.45$ (or $D = 1.1$), while for the top curve $\alpha = 0.40$ (or $D = 1.2$). Enhancement of the critical load compared to that of the smooth crack attains 20.8 % for fractal with $\alpha = 0.40$ and 8.9% for fractal with $\alpha = 0.45$

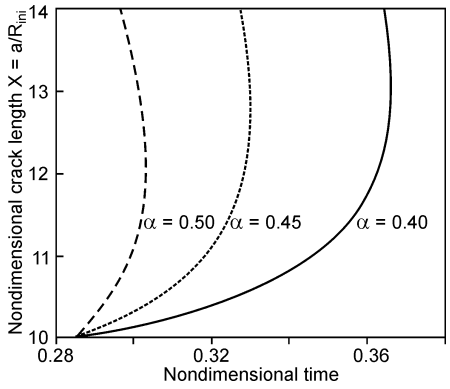

Fig. 13. Crack length shown as a function of nondimensional time parameter for a smooth crack ($\alpha = 0.5$) and two fractal cracks ($\alpha = 0.45$ and 0.40). It is seen that the increased roughness of the crack surfaces leads to a more pronounced quasi-static crack growth. Onset of growth process occurs at a certain threshold of the applied load $\beta_{min} = 0.285$, and it continues until the slopes of the curves approach infinity

where the cohesive zone length R^{f} associated with a fractal crack is related to R for the smooth crack by this expression, cf. Khezrzadeh et al. [44]

$$
\begin{aligned}
&R^{\mathrm{f}} = N(\alpha, X, Y)R,\\
&\delta_{\mathrm{tip}}^{\mathrm{f}} = \kappa(\alpha)\delta_{\mathrm{tip}},\\
&N(\alpha, X, Y) = N_1(\alpha)\beta(X)^{1/\alpha-2},\\
&N_1(\alpha) = 4\pi^{\frac{1}{2\alpha}-2}\left[\frac{\alpha\Gamma(\alpha)}{\Gamma(1/2+\alpha)}\right]^{1/\alpha} \approx\\
&\quad \approx -0.829\alpha^3 + 1.847\alpha^2 - 1.805\alpha + 1.544,\\
&\beta(X) = \frac{2}{\pi}\left(\frac{2Y(X)}{X}\right)^{1/2}
\end{aligned}
\tag{54}
$$

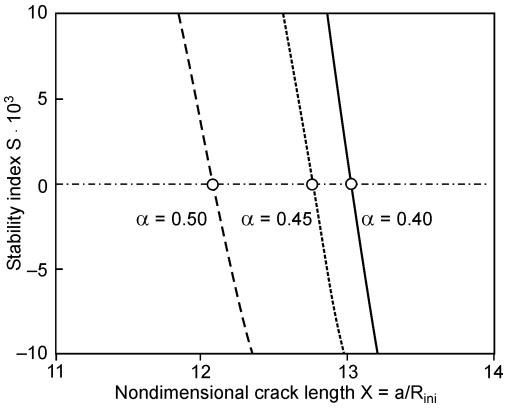

Fig. 12. Stability indices shown as functions of the current crack length for a smooth crack and two fractal (rough) cracks. Intersection points of the S-curves with the horizontal line drawn at $S = 0$ indicate the location of the terminal instability states resulting for a given degree of fractality. Enhancement in the terminal crack length compared to the result valid for a smooth crack is 7.77 % for a fractal crack described by $\alpha = 0.40$ and 5.53 % for a fractal with $\alpha = 0.45$

and the function κ is defined as follows

$$
\kappa(\alpha) = \frac{1 + (\alpha - 1)\sin(\pi\alpha)}{2\alpha(1-\alpha)}. \tag{55}
$$

When all these expressions are substituted into the formula for the vertical component of the displacement within the cohesive zone associated with a fractal crack (53), and when the "final stretch" criterion for the subcritical crack (32) is applied within the restrictions of the Barenblatt's condition $R \ll a$, the following differential equation results

$$
\begin{aligned}
\frac{\mathrm{d}R}{\mathrm{d}a} = \frac{1}{N(\alpha, X, Y)}\{&M(\rho) - 1/2 -\\
&-1/2\ln\left[4\rho N(\alpha, X, Y)R/R_{\mathrm{ini}}\right]\}.
\end{aligned}
\tag{56}
$$

Numerical integration of this equation yields the material resistance curves $R = R(a)$ and the beta-curves shown respectively in Figs. 10 and 11. The plots of stability indices corresponding to each value of the exponent α are shown in Fig. 12. All figures have been drawn at the ductility index $\rho = 20$ and the initial crack length $X_0 = 10$. Finally, diagrams depicted in Fig. 13 show the crack length as a function of time in an analogous way to the results presented in Fig. 4 (for cracks in viscoelastic media) and in Fig. 9 (for smooth cracks embedded in ductile solids).

It is seen that the effect of the roughness of the crack surfaces on the process of slow stable crack growth is substantial. Rougher surfaces of a propagating crack tend to enhance the process of the slow stable crack growth, which precedes onset of the catastrophic fracture.

4. Conclusions

Effects of two parameters on enhancement of the time-dependent fracture manifested by a slow stable crack propa-

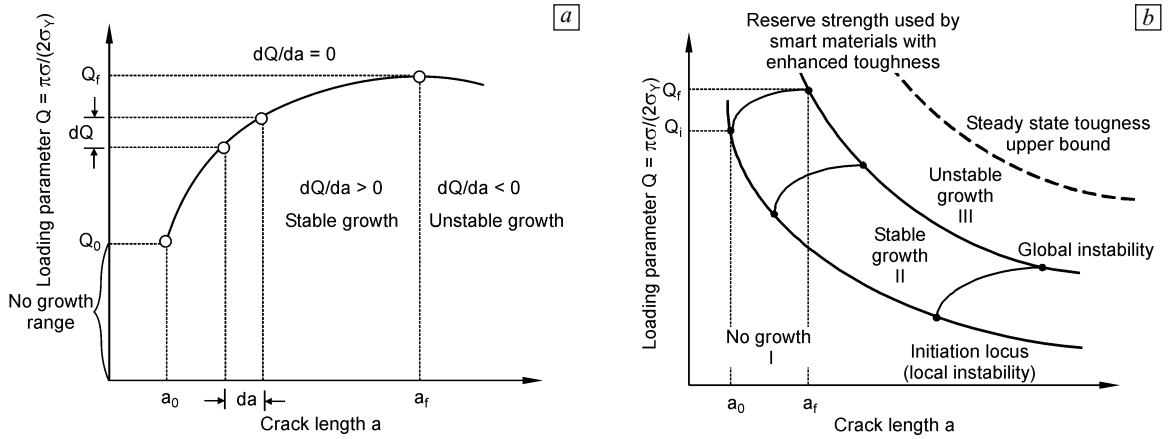

Fig. 14. Phases of crack development in a thick-wall welded pressure vessel (*a*), three ranges of crack growth in ductile solids (*b*): I — no growth region, II — stable quasi-static growth range of load, III — unstable growth (catastrophic fracture)

gation that precedes catastrophic failure in ductile materials have been studied. One of these parameters is related to the material ductility ρ and the other describes the geometry (roughness) of crack surface and is measured by the degree of fractality represented by the fractal exponent α, or — equivalently — by the fractal dimension *D*. These studies of early stages of ductile fracture were preceded by a brief summary of modeling of the phenomenon of delayed fracture in polymeric materials, sometimes referred to as "creep rupture". Despite different physical mechanisms involved in the preliminary stable crack extension and despite different mathematical representations, a remarkable similarity of the end results pertaining to the two phenomena of slow crack growth that occur either in viscoelastic or in ductile media has been demonstrated. For the viscoelastic material the response to the deformation and fracture processes consists in the time-dependent nature of the constitutive equations that play the dominant role in determination of the stable crack extension. For the ductile materials, even though there is no explicit time-dependence in the first principles that govern behavior of these solids, the redistribution of plastic strains in the region adjacent to the front of a propagating crack enables quasi-static continuing crack growth. It has been shown that this process is very similar to a "creeping crack" that propagates through a polymer.

Figure 14 illustrates the three ranges of crack growth, namely, region of no growth (I), region of stable crack extension (II), and region of unstable propagation (III).

Clearly, the existence of the incubation period followed by the propagation phase for a crack embedded in a viscoelastic medium resembles those three growth stages. Our study indicates that both material ductility and geometrical irregularities, such as roughness of the crack surface, enhance the period of slow stable crack extension and substantially influence the characteristics of the terminal instability state attained at the end of the slow crack growth process. For the purpose of fracture prevention both ductility and crack surface roughness are desirable properties.

Appendix

Delayed fracture occurring in a linearly viscoelastic solid such as the one discussed in Sect. 1, consists of two distinct stages: (1) incubation phase, during which the opening displacement associated with the crack increases in time, but the crack remains stationary, and (2) propagation phase, when the crack advances up to the critical length (Griffith length), at which transition to unstable crack extension takes place. Stage I (incubation) is described by the Wnuk–Knauss equation (6) and for the standard linear solid (see Fig. 2) the predicted duration of the incubation phase t_1 is given as

$$t_1 = \tau_2 \ln\left(\frac{\beta_1}{1+\beta_1-n}\right). \tag{A.1}$$

The phase II (crack propagation) is governed by the Mueller–Knauss–Schapery equation (7). For the nondimensional creep compliance function $\Psi(t)$ defined by (12) the resulting equation of motion, which relates crack length x to time t, is given by (24), while the duration of the propagation phase is predicted as follows

$$t_2 = \left(\frac{\tau_2}{\delta}\right)\left\{\frac{n}{1+\beta_1}\ln\left[\frac{\beta_1 n}{1+\beta_1-n}\right] + \ln\left[\frac{1+\beta_1-n}{\beta_1}\right]\right\}. \tag{A.2}$$

The total life time T_{cr} of the component manufactured of a polymeric material that obeys the constitutive equations described in Sect. 1 is obtained as the sum of (A.1) and (A.2), namely

$$T_{cr} = t_1 + t_2 = \tau_2 \ln\left(\frac{\beta_1}{1+\beta_1-n}\right) + \left(\frac{\tau_2}{\delta}\right)\left\{\frac{n}{1+\beta_1}\ln\left[\frac{\beta_1 n}{1+\beta_1-n}\right] + \ln\left[\frac{1+\beta_1-n}{\beta_1}\right]\right\}. \tag{A.3}$$

For Solithane 50/50, a polymer which is used to model mechanical properties of the solid rocket fuel, the times t_1, t_2 and T_{cr} were evaluated by Knauss [45] and Mohanty [28]. The moduli E_1 and E_2 and the viscosity η_2 involved in the standard linear solid that was applied in these studies are as follows

$$E_1 = 6.65\cdot 10^3 \text{ lb/in}^2,\ E_2 = 3.69\cdot 10^3 \text{ lb/in}^2,\quad \eta_2 = 1.36\cdot 10^3 \text{ slb/in}^2. \tag{A.4}$$

This leads to $\beta_1 = 1.8$, the relaxation time $\tau_2 = \eta_2/E_2 = 0.368$ sec and the maximum crack length quotient $n_{max} = 1+\beta_1 = 2.8$. The structural length Δ was estimated as $4.5\cdot 10^{-4}$ inch, while the pre-cut cracks used in the experiments were on the order of 0.225 in. This yielded the inner structural constant $\delta = 2\cdot 10^{-3}$. From (A.4) the "glassy" and the "rubbery" values of the creep compliance function can be readily calculated, namely

$$J_{\text{glassy}} = J(0) = 1.50\cdot 10^{-4}\text{in}^2/\text{lb},\quad J_{\text{rubbery}} = J(\infty) = 4.22\cdot 10^{-4} \text{ in}^2/\text{lb}. \tag{A.5}$$

For detailed calculations the reader is referred to Knauss [45] and Mohanty [28].

The glassy (instantaneous) and rubbery (upon complete relaxation) compliance function values, as given in (A.5), allow one to establish the domains of the delayed fracture, such as "no growth", incubation or the propagation domains. It should be noted that the creep compliance functions involved in these experimental investigations were obtained by use of the Schwarzl and Staverman [46] method, see also Halaunbrenner and Kubisz [47].

In general, the propagation of a crack embedded in the viscoelastic medium will occur within a certain range of applied load. The two limiting values are (1) the Griffith stress evaluated for the initial crack size a_0, which is

$$\sigma_G = \begin{cases} \sqrt{\dfrac{2E\gamma}{\pi a_0}}, \\ \dfrac{K_{IC}}{\sqrt{\pi a_0}} \end{cases} \tag{A.6}$$

and (2) the propagation threshold stress

$$\sigma_{\text{threshold}} = \sqrt{\frac{J(0)}{J(\infty)}}\sigma_G = \sqrt{\frac{J_{\text{glassy}}}{J_{\text{rubbery}}}}\sigma_G. \tag{A.7}$$

For the standard linear solid expression (A.7) reads

$$\sigma_{\text{threshold}} = \frac{1}{\sqrt{1+\beta_1}}\sigma_G. \tag{A.8}$$

Using these relations one can predict the range of the applied loads for a successful delayed fracture test performed on Solithane 50/50 as being between 6/10 of the Griffith stress and the Griffith stress itself.

Summarizing, for the loads below the threshold stress given in (A.7) and (A.8) one enters the "no growth" domain, where propagation does not take place and the cracks in this region remain dormant. The other extreme is attained when the applied constant stress σ_0 reaches the Griffith level σ_G. When σ_0 approaches the Griffith stress we observe an instantaneous fracture as in a brittle medium with no delay effects. Therefore, one may conclude that the delayed fracture occurs only in the range

$$\sigma_{\text{threshold}} \le \sigma_0 \le \sigma_G,\ \frac{\sigma_G}{\sqrt{1+\beta_1}} \le \sigma_0 \le \sigma_G. \tag{A.9}$$

The second expression in (A.9) pertains to the standard linear model.

Let us now consider a numerical example for a polymer characterized by the following properties $\beta_1 = 10$, $\tau_2 = 1$ s and $\delta = 10^{-4}$. Pertinent calculations are performed for three levels of the applied load, measured either by the crack length quotient n $(= \sigma_G^2/\sigma_0^2)$ or by the load ratio $s = \sigma_0/\sigma_G$, namely $n = 8.16$ ($s = 0.35$), $n = 6.25$ ($s = 0.40$) and $n = 4$ ($s = 0.50$). Applying (A.1) and (A.2) we obtain the following incubation t_1 and time-to-failure t_2 values

$$\begin{aligned} &n = 8.16,\ s = 0.35,\ t_1 = 1.26 \text{ s},\\ &t_2 = (1/10^{-4})(0.277)\text{s} = 46.2 \text{ min},\\ &n = 6.25,\ s = 0.40,\ t_1 = 0.744 \text{ s},\\ &t_2 = (1/10^{-4})(0.720)\text{s} = 120 \text{ min},\\ &n = 4,\ s = 0.50,\ t_1 = 0.375 \text{ s},\\ &t_2 = (1/10^{-4})(1.232)\text{s} = 205 \text{ min}. \end{aligned} \tag{A.10}$$

It is noted that for this material the range of the applied stress for the delayed fracture to occur is contained within the interval $(0.3\sigma_G,\ \sigma_G)$. For applied stress less than the threshold stress of $0.3\sigma_G$ the phenomenon of delayed fracture vanishes, and the crack remains stationary.

For ductile solids there are no time-dependent moduli present in the constitutive equations. Yet, the process of quasi-static continuing crack growth does manifest itself as "slow crack growth", which in almost all cases precedes the terminal instability state tantamount to the catastrophic fracture. To understand this phenomenon it is essential to view each instant in the crack growth process as a state of the equilibrium maintained between the applied external effort, say the driving force G or the Rice's J-integral or the stress intensity factor K_I, and the material resistance to crack propagation designated by the index R. In mathematical terms this statement reads

$$G(\sigma, a) = G_R(a),\ J(\sigma, a) = J_R(a),\quad K_I(\sigma, a) = K_R(a). \tag{A.11}$$

Both measures of the external effort G and J are defined in the well-known manner; $J = G = K_I^2/E_1$, while the entities on the right hand sides of (A.11) are defined by the governing equations (37) for a smooth crack and by (56) for a fractal crack. According to Wells the J-criterion for fracture may be replaced by an equivalent COD (or δ_{tip}) criterion — just as it is predicted for the structured cohesive crack model, see Eqs. (42). In this way all expressions

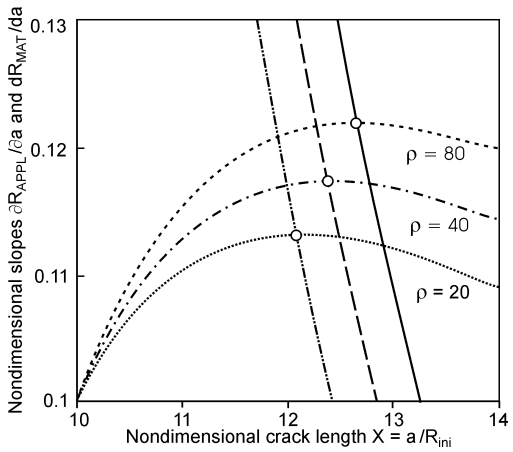

Fig. A1. The nearly straight lines depict the functional relationship between the slope of the material R-curve, $(\mathrm{d}Y/\mathrm{d}X)_{\mathrm{MAT}}$ and the crack length X, while the other set of curves represents the measure of externally applied effort $(Y/X)_{\mathrm{APPL}}$. Points of intersection between these curves designate the terminal instability states, cf. Fig. 8

in (A.11) may be replaced by just a single relation

$$R_{\mathrm{APPL}}(\sigma, a) = R_{\mathrm{MAT}}(a). \tag{A.12}$$

For simplicity the symbol $R_{\mathrm{MAT}}(a)$ is represented in Sect. 2 and 3 by $R(a)$ — or in its nondimensional version — by $Y(X)$. In this way the equilibrium length of the cohesive zone R serves as a measure of the external effort

$$R(\sigma, a) = \frac{1}{2}\left(\frac{\pi\sigma}{2\sigma_Y}\right)^2 a. \tag{A.13}$$

This is a well-known expression resulting for the small-scale yielding case (when the Barenblatt's condition, $R \ll a$, holds) from the Dugdale model. During the slow crack growth phase the quantity defined by (A.13) must be equal R_{MAT} defined by the governing differential equations, either (37) for a smooth crack or (56) for a fractal crack. Attainment of the terminal instability state requires that two conditions are satisfied simultaneously

$$\begin{aligned} &R_{\mathrm{APPL}}(\sigma, a) = R_{\mathrm{MAT}}(a), \\ &\frac{\partial R_{\mathrm{APPL}}(\sigma, a)}{\partial a} = \frac{\mathrm{d}R_{\mathrm{MAT}}(a)}{\mathrm{d}a}. \end{aligned} \tag{A.14}$$

It should be noted that the derivative in the second expression of (A.14) is proportional to the second derivative of the total potential of the system, namely

$$\frac{\partial R_{\mathrm{APPL}}(\sigma, a)}{\partial a} \sim -\frac{\partial^2 \Pi(\sigma, a)}{\partial a^2}. \tag{A.15}$$

Using (42) and recalling that the J-integral equals $-\mathrm{d}\Pi/\mathrm{d}(2a)$ one can readily provide a constant of proportionality between R_{APPL} and the J-integral and their derivatives, which appear in (A.15). The potential of the cracked body $\Pi(\sigma, a)$ is defined as follows

$$\Pi(\sigma, a) = 1/2 \int_V \sigma_{ij}\varepsilon_{ij}\mathrm{d}V - \int_{S_T} T_i u_i \mathrm{d}S - SE(a). \tag{A.16}$$

Symbol $SE(a)$ denotes the surface energy term introduced by Griffith. Using (A.13) we evaluate the derivative needed in (A.14)

$$\begin{aligned} \frac{\partial R_{\mathrm{APPL}}(\sigma, a)}{\partial a} &= \frac{\partial}{\partial a}\left[\frac{1}{2}\left(\frac{\pi\sigma}{2\sigma_{\mathrm{Y}}}\right)^2 a\right] = \\ &= \frac{1}{2}\left(\frac{\pi\sigma}{2\sigma_{\mathrm{Y}}}\right)^2 = \frac{R_{\mathrm{APPL}}}{a} = \frac{Y}{X}. \end{aligned} \tag{A.17}$$

At the terminal instability point this expression should equal the derivative $\mathrm{d}Y/\mathrm{d}X$ defined in (37) and/or (56), namely

$$\left[\frac{\mathrm{d}Y}{\mathrm{d}X}\right]_{\mathrm{transition}} = \left(\frac{Y}{X}\right)_{\mathrm{transition}}. \tag{A.18}$$

The index "transition" refers to the attainment of the terminal instability state, which is tantamount to the transition from stable to unstable crack propagation. It is noted that the condition (A.18) is exactly equivalent to the requirement that the stability index defined in (50) equals zero. Figure A1 illustrates how the condition (A.18) may be used to determine the state of the terminal instability. The intersection points shown in Fig. A1 coincide exactly with the results obtained in Sect. 2 for a smooth crack for three different levels of the material ductility, cf. Fig. 8.

In an analogous way the case of the fractal crack can be resolved. Here one has

$$\begin{aligned} &\frac{\partial R^{\mathrm{f}}_{\mathrm{APPL}}}{\partial a} = \frac{R^{\mathrm{f}}_{\mathrm{APPL}}}{\partial a} = N(\alpha, X, Y)\frac{R_{APPL}}{a} = \\ &= N(\alpha, X, Y)\frac{Y}{X}, \\ &\frac{\mathrm{d}R^{\mathrm{f}}_{\mathrm{MAT}}}{\mathrm{d}a} = N(\alpha, X, Y)\frac{\mathrm{d}Y}{\mathrm{d}X}. \end{aligned} \tag{A.19}$$

When these two entities representing the rate of the external effort and the rate of material resistance to continuing crack extension, the factor $N(\alpha, X, Y)$ cancels out, and one recovers the condition for the terminal instability expressed by (A.18).

References

[1] S.N. Zhurkov, Kinetic concept of the strength of solids, Int. J. Fracture, 1 (1965) 311.
[2] S.N. Zhurkov and T.P. Sanfirova, A study of the time and temperature dependence of mechanical strength, Soviet Solid State Physics, 2 (1960) 933.
[3] W.G. Knauss, The time dependent fracture of viscoelastic materials, in *Proc. First Int. Conf. Fracture*, 2 (1965) 1139.
[4] J.R. Willis, Crack propagation in viscoelastic media, J. Mech. Phys. Solids, 15 (1967) 229.
[5] M.L. Williams and R.A. Schapery, Spherical flaw instability in hydrostatic tension, Int. J. Fracture, 1 (1967) 64.
[6] M.L. Williams, The kinetic energy contribution to fracture propagation in a linearly viscoelastic material, Int. J. Fracture, 4 (1966) 69.
[7] M.L. Williams, The continuum interpretation for fracture and adhesion, J. Appl. Polymer Science, 13 (1969) 29.
[8] M.P. Wnuk and W.G. Knauss, Delayed fracture in viscoelastic-plastic solids, Int. J. Solids Struct., 6 (1970) 995.

[9] F.A. Field, A simple crack extension criterion for time-dependent spallation, J. Mech. Phys. Solids, 19 (1971) 61.
[10] M.P. Wnuk, Energy criterion for initiation and spread of fracture in viscoelastic solids, Engineering Experimental Station Bulletin, 7 (1968).
[11] M.P. Wnuk, Effects of time and plasticity on fracture, British J. Appl. Physics, 2, Ser. 2 (1969) 1245.
[12] M.P. Wnuk, Energy criterion for initiation and spread of fracture in viscoelastic solids, Tech. Report of Eng. Experimental Station at SDSU, 7 (1968).
[13] M.P. Wnuk, Nature of fracture in relation to the total potential energy, British J. Appl. Physics, 1, Ser. 2 (1968) 217.
[14] M.P. Wnuk, Similarity between creep rupture in viscoelastic solids and fatigue in metals (inelastic fatigue), SDSU Technical Report No. 1 for the Office of Naval Research, 1970.
[15] M.P. Wnuk, Delayed fracture under alternating loadings, SDSU Tech. Report No. 2 for the Office of Naval Research, 1970.
[16] M.P. Wnuk, Prior-to-failure extension of flaws under monotonic and pulsating loadings, SDSU Tech. Report No. 3, Engineering Experimental Station Bulletin at SDSU, Brookings, SD, 1971.
[17] M.P. Wnuk, Accelerating Crack in a Viscoelastic Solid Subject to Subcritical Stress Intensity, in *Proc. Int. Conf. on Dynamic Crack Propagation*, Ed. by G.C. Sih, Noordhoff, Leyden, Netherlands (1972) 273.
[18] W.G. Knauss and H. Dietmann, Crack propagation under variable load histories in linearly viscoelastic solids, Int. J. Engineering Science, 8 (1970) 643.
[19] H.K. Mueller and W.G. Knauss, Crack propagation in a linearly viscoelastic strip, J. Appl. Mech. E., 38 (1971) 483.
[20] H.K. Mueller and W.G. Knauss, The fracture energy and some mechanical properties of a polyurethane elastomer, Trans. Soc. Rheol., 15 (1971) 217.
[21] G.A.C. Graham, The correspondence principle of linear viscoelasticity theory for mixed boundary value problems involving time dependent boundary regions, Q. Appl. Math., 26 (1968) 167.
[22] G.A.C. Graham, The solution of mixed boundary value problems that involve time-dependent boundary regions for viscoelastic materials with one relaxation function, Acta Mechanica, 8 (1969) 188.
[23] B.V. Kostrov and L.V. Nikitin, Some general problems of mechanics of brittle fracture, Archiwum Mechaniki Stosowanej, 22 (1970) 749.
[24] H.K. Mueller, Stress-intensity factor and crack opening for a linearly viscoelastic strip with a slowly propagating central crack, Int. J. Fracture, 7 (1971) 129.
[25] W.G. Knauss, The mechanics of polymer fracture, Appl. Mechanics Reviews, 26 (1973) 1.
[26] R.A. Schapery, A theory of crack growth in viscoelastic media, Int. J. Fracture, 11 (1973) 141.
[27] M.P. Wnuk, Quasi-static extension of a tensile crack contained in a visco-plastic solid, J. Appl. Mech., 11 (1974) 141.
[28] D. Mohanty, Experimental study of viscoelastic properties and fracture characteristics in polymers, M.S. Thesis at Dept. of Mechanical Engineering, South Dakota State University, Brookings, SD, 1972.
[29] M.P. Wnuk and T. Mura, Stability of a disc-shaped geothermal reservoir subjected to hydraulic and thermal loadings, Int. J. Fracture, 17, No. 5 (1981) 493.
[30] M.P. Wnuk and T. Mura, Effect of microstructure on the upper and lower limit of material toughness in elastic-plastic fracture, Mechanics of Materials, 2 (1983) 33.
[31] J.R. Rice, Mathematical Analysis in the Mechanics of Fracture, in *Fracture. An advanced Treatise*, V. II, Ed. by H. Liebowitz, Academic Press, New York, 1968.
[32] J.R. Rice, Thermodynamics of the quasi-static growth of Griffith crack, J. Mech. Phys. of Solids, 26 (1978) 61.
[33] J.R. Rice and E.P. Sorensen, Continuing crack-tip deformation and fracture for plane strain crack growth in elastic-plastic solids, J. Mech. Phys. Solids, 26 (1978) 163.
[34] J.R. Rice, W.J. Drugan, and T.L. Sham, Elastic-plastic analysis of growing cracks, in *Fracture Mechanics: 12th Conference*, ASTM STP 700 (1980) 189–221.
[35] A. Wells, Application of fracture mechanics at and beyond general yielding, Brit. Weld. J., 10 (1963) 563.
[36] A. Rouzbehani and M.P. Wnuk, Instabilities in early stages of ductile fracture, Phys. Mesomech., 8, No. 5–6 (2005) 81.
[37] M.P. Wnuk, Enhancement of Fracture Toughness due to Energy Screening Effect in the Early Stages of Non-elastic Failure, in *Fatigue and Fracture of Engineering Materials*, Blackwell Publishing Ltd., UK, 26 (2003) 741.
[38] M.P. Wnuk, Mesomechanics of quasi-static fracture, Phys. Mesomech., 6, No. 4 (2003) 85.
[39] M.P. Wnuk, Quantum theory of quasi-static fracture propagating in nonelastic solids, Maintenance and Reliability – Reports of Tech. University of Lublin, 2 (2003) 6.
[40] M.P. Wnuk and A. Yavari, On estimating stress intensity factors and modulus of cohesion for fractal cracks, Eng. Fract. Mech., 70 (2003) 1659.
[41] M.P. Wnuk and A. Yavari, A correspondence principle for fractal and classic cracks, Eng. Fract. Mech., 72 (2005) 2744.
[42] M.P. Wnuk and A. Yavari, Discrete fractal fracture mechanics, Eng. Fract. Mech., 75 (2008) 1127.
[43] M.P. Wnuk and A. Yavari, A discrete cohesive model for fractal cracks, Eng. Fract. Mech., 76 (2009) 548.
[44] H. Khezrzadeh, M.P. Wnuk, and A. Yavari, Influence of material ductility and crack surface roughness on fracture instability, J. Appl. Physics D, 44 (2011) 395302.
[45] W.G. Knauss, Stable and unstable crack growth in viscoelastic media, Trans. Soc. Rheol., 13 (1969) 291.
[46] F. Schwarzl and A.J. Staverman, Higher approximations of relaxation spectra, Physica, 18 (1952) 791.
[47] J. Halaunbrenner and A. Kubisz, Contact region of a hard ball rolling on a viscoelastic plate, J. Appl. Mech. F, 90, No. 1 (1968) 102.